



CrossMark  
click for updates

Cite this: *RSC Adv.*, 2015, 5, 52543

# Comparative investigation of spectroelectrochemical and biosensor application of two isomeric thienylpyrrole derivatives

Rukiye Ayranci,<sup>a</sup> Tugba Soganci,<sup>a</sup> Merve Guzel,<sup>a</sup> Dilek Odaci Demirkol,<sup>\*bc</sup> Metin Ak<sup>\*a</sup> and Suna Timur<sup>bc</sup>

In the present work, we performed a comparative investigation of spectroelectrochemical and biosensor application of isomeric thienylpyrrole derivatives. For this purpose two thienylpyrrole derivatives were synthesized characterized and electrochemically polymerized. Characterizations of the resulting polymers were performed by cyclic voltammetry (CV), UV-vis spectroscopy. Moreover, the spectroelectrochemical, electrochromic properties and biosensing applications of the polymer films were investigated. The resulting polymer films have distinct electrochromic properties and show five different colors. The 4-(2,5-di(thiophen-2-yl)-1*H*-pyrrol-1-yl)aniline (SNS-NH<sub>2</sub>) and 3-(2,5-di(thiophen-2-yl)-1*H*-pyrrol-1-yl)aniline P(SNS-*m*NH<sub>2</sub>) films show maximum optical contrast ( $\Delta T\%$ ) of 41.5%, 25.4% at 431 nm, 422 nm with a response time of 1.5 s. For biosensing studies, P(SNS-NH<sub>2</sub>) and P(SNS-*m*NH<sub>2</sub>) were polymerized on graphite electrodes electrochemically and used as immobilization matrices. After electrochemical deposition, glucose oxidase (GOx) was immobilized on the modified electrodes as the model enzyme. Effects of the position of the amine group on spectroelectrochemical properties and biosensing capability of the polymers were investigated.

Received 21st April 2015

Accepted 8th June 2015

DOI: 10.1039/c5ra07247f

[www.rsc.org/advances](http://www.rsc.org/advances)

## 1. Introduction

Conjugated polymers (CPs) include a  $\pi$ -electron backbone in charge of their unconventional electronic properties such as electrical conductivity, high electron affinity, low ionization potential and low energy optical transitions. These extensive  $\pi$ -conjugated systems of the CPs have double and single bonds alternating along the polymer chain. These materials are especially attractive because they show magnetic, electrical and optical properties of semiconductors or metals while retaining the desirable mechanical properties and processing advantages of polymers. Their unconventional electronic and optical properties have made them very appealing materials in various applications including solar cells, light weight batteries, electrochromic devices, molecular electronic devices and sensors.<sup>1,2</sup> Over the past 30 years, the conducting polymers belonging to polyenes or polyaromatics such as polyaniline, polypyrrole, polythiophene, poly(*p*-phenylene) have attracted most attention.<sup>3,4</sup> Between the CPs polythiophene and polypyrrole are of exclusive interest because of their high conductivity, interesting

redox properties, stability in the oxidized state and simplicity and accessibility of the preparation of the starting monomers.<sup>6-9</sup> Many authors carried out synthesis of substituted and unsubstituted 2,5-di(2-thienyl)pyrroles and the study of their electrochemical behavior.<sup>10-14</sup>

Lately, CPs have attracted much attention in the development of biosensors.<sup>15-17</sup> For immobilization of biomolecules, CP serve as a suitable matrix supplying widespread properties.<sup>18</sup> Their high reproducibility, easy preparation, electrochemical properties and compatibility with biological molecules make them fascinating in biosensor design. CPs are also known to have superior properties, which allow them to act as excellent materials for biomolecule immobilization and rapid electron transfer for the fabrication of efficient biosensors.<sup>19-22</sup> CP interfaces are especially convenient for situating biomolecules onto micro sized surfaces.<sup>4</sup> Also, conducting polymers offers the facility to modulate their electronic properties *via* molecular interactions. Many investigators have demonstrated that covalent functionalization of conducting polymers could be obtained by synthesis of functionalized monomers bearing a prosthetic group, which are subsequently polymerised.<sup>5</sup> The progress of such systems strongly depends on efficient protein immobilization on polymer substrates. In order to reach this complex heterogeneous interaction the polymer surface must be functionalized with chemical groups that are reactive towards proteins in a way that surface functional groups (such as carboxyl, -COOH; amine, -NH<sub>2</sub>; and hydroxyl, -OH)

<sup>a</sup>Pamukkale University, Faculty of Art and Science, Chemistry Department, Denizli, Turkey. E-mail: [metinak@pau.edu.tr](mailto:metinak@pau.edu.tr)

<sup>b</sup>Ege University, Faculty of Science, Biochemistry Department, 35100 Bornova, Izmir, Turkey

<sup>c</sup>Ege University, Institute of Drug Abuse Toxicology & Pharmaceutical Sciences, 35100, Turkey

chemically or physically anchor the proteins to the polymer platform.<sup>23</sup>

Glucose analysis is crucial in the clinical chemistry as well as in fermentation and food industries. Many articles have been published on this subject.<sup>24–27</sup> Plenty of the primordial glucose biosensors were established on H<sub>2</sub>O<sub>2</sub> produced in the enzymatic oxidation of glucose by glucose oxidase (GOx) or amperometric determination of consumed oxygen.<sup>5</sup> Electrochemical amperometric biosensors are widely used class of glucose biosensing.<sup>28,29</sup> Fabrications of amperometric biosensors are rely on the electroactivity of the substrate or the product of the enzymatic reaction (first generation biosensors). First-generation glucose biosensors based on the use of the natural oxygen co-substrate and generation and detection of H<sub>2</sub>O<sub>2</sub>. Recently Krikstolaityte *et al.* study on enzymatic polymerization of polythiophene by immobilized glucose oxidase.<sup>30</sup> Then Ramanavicius *et al.* reported on electrochemical impedance spectroscopy based evaluation of 1,10-phenanthroline-5,6-dione and glucose oxidase modified graphite electrode.<sup>31</sup>

GOx is widely used in glucose biosensing. In the presence of molecular oxygen, GOx catalyzes the oxidation of β-D-glucose to hydrogen peroxide and glucono-δ-lactone which is subsequently hydrolyzed into gluconic acid.<sup>32</sup>

In this paper, we report the synthesis and characterization of electronic properties of SNS-NH<sub>2</sub> and SNS-*m*NH<sub>2</sub>. Furthermore, glucose biosensor platforms were constructed which is based on covalent immobilization of glucose oxidase on P(SNS-NH<sub>2</sub>) and P(SNS-*m*NH<sub>2</sub>) modified electrode. Enzyme immobilization platforms were investigated as first generation glucose sensor. Effect of the position of the amine group on spectroelectrochemical properties and biosensing capability of polymers were investigated.

## 2. Experimental

### 2.1 Chemicals

Thiophene (C<sub>4</sub>H<sub>4</sub>S), toluene (C<sub>7</sub>H<sub>8</sub>), succinyl chloride (C<sub>4</sub>H<sub>6</sub>Cl<sub>2</sub>O), hydrochloric acid (HCl), sodiumbicarbonate (NaHCO<sub>3</sub>), magnesiumsulphate (MgSO<sub>4</sub>), ethanol (C<sub>2</sub>H<sub>4</sub>OH), propionic acid (C<sub>3</sub>H<sub>6</sub>O<sub>2</sub>), (TBF<sub>6</sub>) were purchased from Aldrich. Pyrrole monomer is commercially available from Alfa Aesar. Dichloromethane (CH<sub>2</sub>Cl<sub>2</sub>) is used as solvent and AlCl<sub>3</sub> supplied from Merck. D-glucose, ethanol, glucose oxidase (GOx, from *Aspergillus niger*, 200 U mg<sup>-1</sup>), glutaraldehyde (25%) were provide from Sigma. All other chemicals were analytical grade.

### 2.2 Instruments

Cyclic voltammetric and amperometric measurements were carried out by Radiometer (Lyon, France, <http://www.radiometer.com>) and Palmsens (Houten, The Netherlands, <http://www.palmsens.com>) electrochemical measurement unit with three electrode systems, respectively. Three-electrode cell geometry was used in all electrochemical experiments. Graphite electrode (Ringsdorff Werke GmbH, Bonn, Germany, 3.05 mm diameter and 13% porosity) was used as the working electrode. Pt and Ag electrodes (Metrohm, Switzerland)

were used as the counter and reference electrodes respectively. All potential values are referred to Ag/Ag<sup>+</sup> (3.0 M KCl, Metrohm, Switzerland) reference electrode.

### 2.3 Synthesis of SNS-NH<sub>2</sub> and SNS-*m*NH<sub>2</sub>

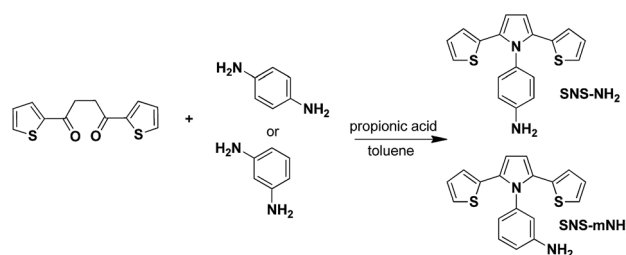
The monomers, SNS-NH<sub>2</sub> and SNS-*m*NH<sub>2</sub>, were synthesized from 1,4-di(2-thienyl)-1,4 butadione and benzene-1,4-diamine or benzene-1,3-diamine in the presence of catalytic amount of propionic acid.<sup>13,33</sup> In the presence of AlCl<sub>3</sub>, 1,4-di(2-thienyl)-1,4 butadione was synthesized with the double Friedel-Crafts reaction. The reaction mixture was refluxed for 4 h. A round-bottomed flask equipped with magnetic stirrer was charged with 1,4-di(2-thienyl)-1,4 butanedione, propionic acid, toluene and corresponding diamine. The resultant mixture was stirred and refluxed for 24 h. Evaporation of the toluene, followed by flash column chromatography (SiO<sub>2</sub> column, elution with dichloromethane), the desired compound as a pale green powder was obtained. The synthetic routes of the monomers are shown in Scheme 1.

### 2.4 Electrochemical polymerization and spectroelectrochemistry

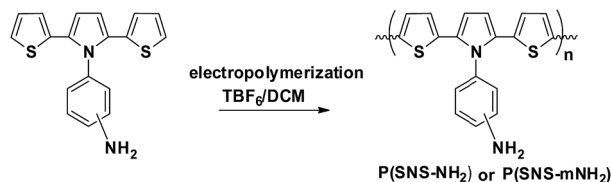
Electrochemical polymerization of SNS-NH<sub>2</sub> and SNS-*m*NH<sub>2</sub> were carried out by potentiodynamically sweeping the potential between -0.5 to 1.5 V at 250 mV s<sup>-1</sup> in the presence of 0.01 M corresponding diamine (0.01 M) and 0.05 M TBF<sub>6</sub>/DCM (Scheme 2). The system consist of a potentiostant a CV cell containing ITO working electrode, platinum wire counter electrode and Ag wire as a pseudo reference electrode. After polymerizations, polymer films were rinsed in DCM to remove monomer residue. Spectroelectrochemical analyses of the polymers were carried out to understand the band structure of the product. In order to carry out the spectroelectrochemical experiments, polymer films were deposited potentiodynamically on ITO-coated glass. UV-vis spectra of the polymers films were recorded at different potentials in TBF<sub>6</sub> (0.05 M)/DCM.

### 2.5 Preparation of enzyme electrodes

Initially, thin polymer films were deposited onto the graphite electrode in 0.05 M TBF<sub>6</sub>/DCM *via* potentiodynamic electrochemical polymerization of monomers (5.0 mg mL<sup>-1</sup>). Before the electropolymerization, a graphite rod was polished on wet emery paper and washed thoroughly with distilled water. For the immobilization of GOx, 2.5 mL enzyme solution (1.0 mg of



Scheme 1 The synthetic route of SNS-NH<sub>2</sub> and SNS-*m*NH<sub>2</sub>.



Scheme 2 Electrochemical synthesis route for P(SNS-NH<sub>2</sub>) and P(SNS-*m*NH<sub>2</sub>).

enzyme was dissolved in 2.5 mL buffer solution which equals to 50 Unit) and 1.0% of 2.5 mL glutaraldehyde (GA) in sodium acetate buffer (50 mM, pH 7.0) were dropped on the electrode. The electrodes were dried at the ambient conditions for 2 h.<sup>34</sup>

## 2.6 Measurement of the sensor response

Cyclic voltammetry studies of enzyme electrodes were carried out in 10 mL Na-acetate buffer (0.05 M, pH 4.5) under potential between  $-0.5$ – $1.5$  V at the scan rate of  $250$  mV s<sup>-1</sup>. Chronoamperometric measurements for the first generation biosensors were performed in Na-acetate buffer. Before and after glucose addition, current densities were recorded at  $+0.45$  V vs. Ag<sup>+</sup>/AgCl reference electrode and the current vs. time plot has been obtained. Each measurement was carried out at least 3 times.

## 3. Result and discussion

### 3.1 Electrochemical properties of P(SNS-NH<sub>2</sub>) and P(SNS-*m*NH<sub>2</sub>)

The redox behaviors of the (SNS-NH<sub>2</sub>) and (SNS-*m*NH<sub>2</sub>) were investigated by cyclic voltammetry. The CV cell composed of ITO glass slide as working electrode, a platinum wire as counter electrodes and a silver wire pseudo reference electrode. Experiments were performed in TBF<sub>6</sub> (0.05 M)/DCM solvent electrolyte couple at room temperature at  $250$  mV s<sup>-1</sup>. Cyclic voltammogram of (SNS-NH<sub>2</sub>) showed one reduction peak at  $+0.4$  V and one oxidation peak at  $+0.76$  V due to polymer reduction and monomer oxidation when the potential range between  $-0.5$  and  $+1.5$  V was investigated (Fig. 1a). First cycle of (SNS-*m*NH<sub>2</sub>) CV graph shows two oxidation peak at  $+0.53$  V and  $+0.79$  V. The last cycle of voltammogram have peaks at  $+0.63$  V and  $+0.22$  V because of oxidation and reduction of the polymer, (Fig. 1b). Increment in the current density with consecutive cycles implies formation of polymer film on the electrode. The oxidation onset potential of SNS-NH<sub>2</sub> is initiated at  $0.5$  V which is much lower than that of SNS-*m*NH<sub>2</sub> ( $0.65$  V) (Fig. 2). These results indicate that amino group located at the *para* position facilitates oxidation of the monomer.

**3.1.1 Scan rate dependence of the peak currents.** Cyclic voltammograms are most often characterized by the dependence of peak currents ( $i_p$ ) on the scan rate ( $\nu$ ). In respect of electrochemical experiments, for a behavior dominated by diffusion effects,  $i_p$  is proportional to  $\nu^{1/2}$ , while for a material deposited on the electrode surface, such as a CP film,  $i_p$  is proportional to  $\nu$ . However, this is so only for conducting

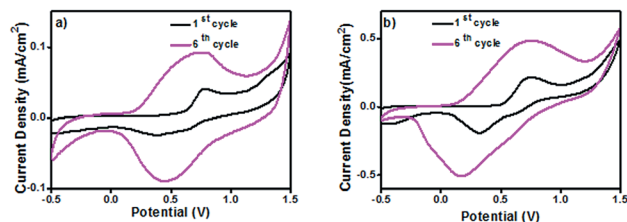


Fig. 1 Cyclic voltammograms of (a) (SNS-NH<sub>2</sub>), (b) (SNS-*m*NH<sub>2</sub>) in TBFE/DCM by sweeping the potential between  $0.5$  and  $1.5$  V at  $250$  mV s<sup>-1</sup>.

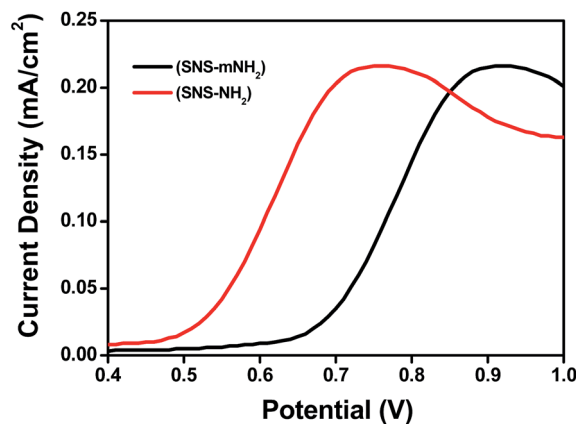


Fig. 2 Anodic polarization curves of SNS-NH<sub>2</sub> and SNS-*m*NH<sub>2</sub>.

polymer films that are not extraordinarily thick, not extraordinarily compact and not doped with bulky dopant ions which have extraordinarily small diffusion coefficients. If any of the latter conditions prevail  $i_p$  can be proportional to  $\nu^{1/2}$ .<sup>35</sup>

(SNS-NH<sub>2</sub>) and (SNS-*m*NH<sub>2</sub>) films prepared with CV ( $-0.5$  to  $1.5$  V) and washed with DCM and their cyclic voltammograms were performed in monomer free electrolyte at different scan rates (Fig. 3b insert graph). The anodic and cathodic peak currents show a linear dependence (anodic and cathodic least

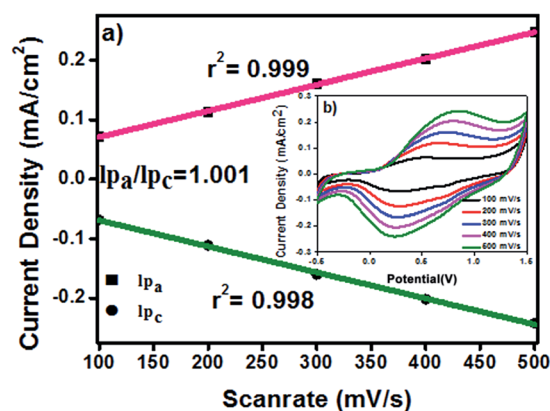


Fig. 3 (a) Dependence scan rate on peak current for P(SNS-NH<sub>2</sub>) ( $i_{pa}$ : anodic peak current value,  $i_{pc}$ : cathodic peak value,  $r^2$ : linear regression value), (b) CV of P(SNS-NH<sub>2</sub>) at different scan rates.

squares fit of  $R = 0.999$ ,  $R = 0.998$ , respectively) as a function of the scan rate as illustrated in (Fig. 3a) for P(SNS-NH<sub>2</sub>).

Fig. 4b inset graph shows cyclic voltammograms of P(SNS-*m*NH<sub>2</sub>) at different scan rates. There is a linear dependence between anodic and cathodic peak currents and scan rate as illustrated in (Fig. 4a). The current responses were directly proportional to the scan rate indicating that the polymer films were electroactive and adhered well to the electrode.<sup>36</sup> The linearities of scan rate dependence with respect to current for the anodic and cathodic peaks are illustrated in insert figure (Fig. 4b). These demonstrate that the electrochemical processes are not diffusion limited even at very high scan rates. On the other hand, polymers exhibit quasi-reversible electrochemical behaviors and chemical reversibility, as evidenced by  $i_{pa}/i_{pc}$  values are equal to unity.

### 3.2 Electrochromic properties of P(SNS-NH<sub>2</sub>) and P(SNS-*m*NH<sub>2</sub>)

**3.2.1 Spectroelectrochemical properties of P(SNS-NH<sub>2</sub>) and P(SNS-*m*NH<sub>2</sub>).** For spectroelectrochemical studies, the polymer film P(SNS-NH<sub>2</sub>) was deposited potentiostatically at 1.5 V from a solution of TBF<sub>6</sub>/DCM onto ITO-coated glass slide. In monomer free TBF<sub>6</sub>/DCM solution, UV spectra of the films were recorded at different potentials. The  $\lambda_{max}$  value for the  $\pi-\pi^*$  transitions in the neutral state of P(SNS-NH<sub>2</sub>) was found to be 431 nm. The electronic band gap ( $E_g$ ) determined as the onset energy for the  $\pi-\pi^*$  transition was found to be 2.09 eV. Fig. 5 shows spectroelectrochemical spectrum of P(SNS-NH<sub>2</sub>) film and colors of the polymer at different applied potentials.

The polymer film P(SNS-*m*NH<sub>2</sub>) was deposited onto transparent electrode (ITO) the same condition as P(SNS-NH<sub>2</sub>). UV spectra of the films were recorded at different potentials in monomer free TBF<sub>6</sub>/DCM solution. The  $\lambda_{max}$  value for the  $\pi-\pi^*$  transitions in the neutral state of P(SNS-*m*NH<sub>2</sub>) was found to be 422 nm, corresponding to yellow color. The electronic band gap defined as the onset energy for the  $\pi-\pi^*$  transition was calculated to 2.17 eV. Fig. 6 indicates optoelectrochemical spectrum of P(SNS-*m*NH<sub>2</sub>) film at applied potentials between 0.4 V and

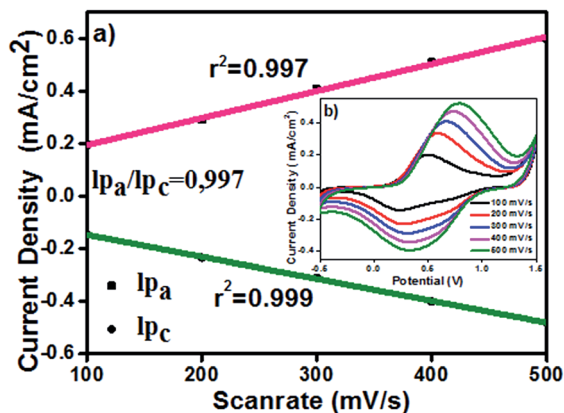


Fig. 4 (a) Dependence scan rate on peak current for P(SNS-*m*NH<sub>2</sub>) ( $i_{pa}$ : anodic peak current value,  $i_{pc}$ : cathodic peak value,  $r^2$ : linear regression value). (b) CV of P(SNS-*m*NH<sub>2</sub>) at different scan rates.

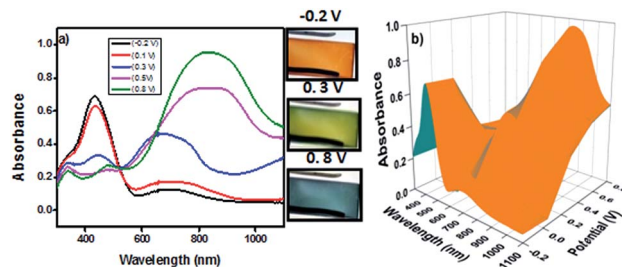


Fig. 5 Optoelectrochemical spectrum of P(SNS-NH<sub>2</sub>) film (a) 2D and (b) 3D.

+1.2 V and colour of the polymer at various applied potentials. Introduction of *p*-amine in the monomer pattern yielded a more electroactive and more conjugated polymer compared with those electrogenerated from the *meta* isomer. As a result band gap decrease and improvement of optical contrast were observed for P(SNS-NH<sub>2</sub>).

**3.2.2 Spectroelectrochemical switching time of the P(SNS-NH<sub>2</sub>) and P(SNS-*m*NH<sub>2</sub>).** The switching time is described as the time elapsed between the lowest and highest transmittance values which were figured out from graph of the transmittance change-time. The switching times of the polymers were determined by monitoring the %*T* change at maximum absorbance through switching the applied potential in a square wave form between -0.5 and 1.5 V with a residence time of 5 s. Applied potentials of the corresponding extreme states of the polymers, were acquired from the optoelectrochemistry studies. As seen in Fig. 7a, P(SNS-NH<sub>2</sub>) has 41.5% and 74.2% optical contrast values at 431 and 834 nm, respectively, with a 1.5 s and 2.0 s switching time. As seen in Fig. 7b, P(SNS-*m*NH<sub>2</sub>) has 25.4% and 54.1% optical contrast values at 422 and 884 nm, respectively, with a 1.48 s and 1.61 switching time.

### 3.3 Biosensor applications

Herein, P(SNS-NH<sub>2</sub>) and P(SNS-*m*NH<sub>2</sub>) were successfully electrochemically polymerized. Polymers were used as matrix for enzyme immobilization owing to the presence of free amino groups. GOx was immobilized on the polymer coated modified graphite electrode surfaces *via* using glutaraldehyde<sup>34</sup> to obtain a consistent immobilization. Cyclic voltammetry, calibration curve and optimum pH studies for the prepared biosensor were done.

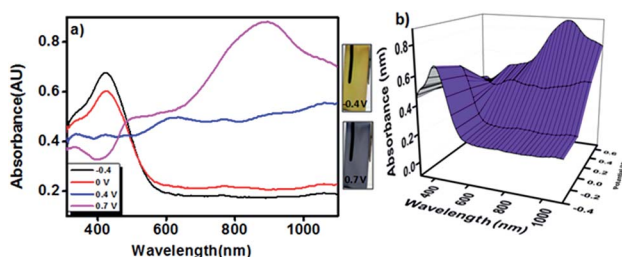


Fig. 6 Optoelectrochemical spectrum of P(SNS-*m*NH<sub>2</sub>) film (a) 2D and (b) 3D.

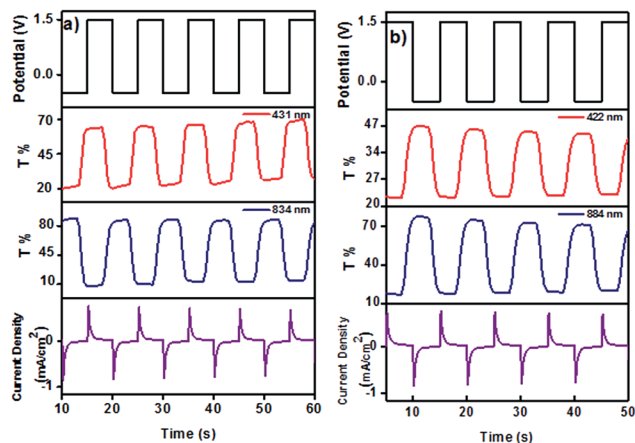


Fig. 7 Potential, absorbance and current density versus-time graphs of P(SNS-NH<sub>2</sub>) (a) and P(SNS-mNH<sub>2</sub>) (b).

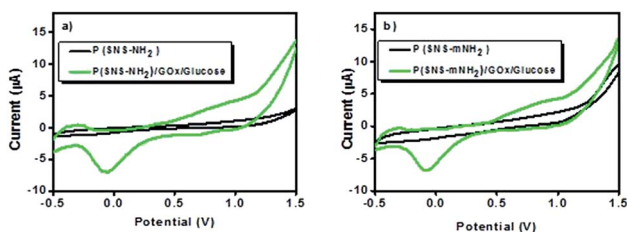


Fig. 8 CVs of (a) P(SNS-NH<sub>2</sub>), P(SNS-NH<sub>2</sub>)/GOx/glucose (b) P(SNS-mNH<sub>2</sub>), P(SNS-mNH<sub>2</sub>)/GOx/glucose (Na-acetate buffer pH 4.5, 50 mM at 250 mV per scan rate).

For this purpose, CV was used to characterize the assembly process of the modified electrode. Cyclic voltammograms of SNS-NH<sub>2</sub>, SNS-NH<sub>2</sub>/GOx/Glucose which have been determined at scan rate of 250 mV in Na-Acetate buffer between -0.5 V and 1.8 V shown in Fig.8. An apparent increase in oxidation and reduction peak currents were realized after SNS-NH<sub>2</sub>/GOx and SNS-mNH<sub>2</sub>/GOx were coated on the electrode, meaning that biosensors have good conductivity and can facilitate the electron transfer in the presence of glucose. Monomer that comprises a group with primer amine (NH<sub>2</sub>) functionality for covalent immobilization of biomolecule to the electrode surface caused increase redox currents.

Optimum pH and calibration curves were determined for the polymers. The working at correct pH values in biosensors is

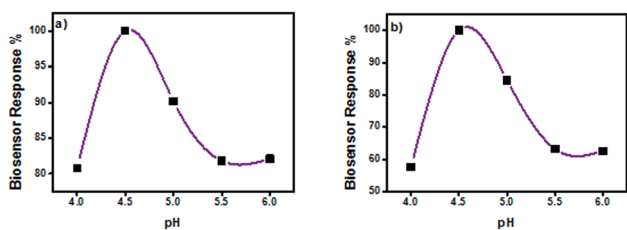


Fig. 9 Effect of pH (a) P(SNS-NH<sub>2</sub>)/GOx (b) P(SNS-mNH<sub>2</sub>)/GOx (in Na-acetate buffer, 50 mM, at pH 4.0–6.0 and in sodium phosphate buffer; +0.45 V, [Glc]: 5.0 mM).

important to tracked enzyme activity or biosensor response to substrates. pH values of working buffer affects on the nature of immobilization matrix which contains positively or negatively charged groups. Relative response values of P(SNS-NH<sub>2</sub>)/GOx and P(SNS-mNH<sub>2</sub>)/GOx biosensors achieved maximum at pH 4.50 (Fig. 9).

Current density of substrate concentration has been investigated and calibration curves has been generated for enzyme electrode constructed by P(SNS-NH<sub>2</sub>)/GOx and P(SNS-mNH<sub>2</sub>)/GOx. For that reason, amperometric responses of constructed enzyme electrodes have been plotted comparatively in Fig. 10. Biosensor responses for both polymers were calculated in terms of current (in µA cm<sup>-2</sup>) at different glucose concentrations from 0 to 10 mM by measuring chronoamperometry method at +0.45 V. A linear relationship was obtained between substrate concentration (x) and biosensor response (y) with the equation of  $y = 0.182x + 0.736$  ( $R = 0.997$ ) for P(SNS-NH<sub>2</sub>)/GOx and  $y = 0.387x + 0.658$  ( $R = 0.984$ ) for P(SNS-mNH<sub>2</sub>)/GOx. After these results, a middle value has been chosen in the region detected as linear (5.0 mM) and this value has been utilized for repeatability of the analysis results for (SNS-NH<sub>2</sub>)/GOx biosensor. These results show that biosensor response of P(SNS-NH<sub>2</sub>) is much higher than P(SNS-mNH<sub>2</sub>). We believe that this result is due to steric effect that crosslinking procedures more favourable between glutaraldehyde and P(SNS-NH<sub>2</sub>) to obtain a stable immobilization.

For P(SNS-NH<sub>2</sub>)/GOx enzyme sensor constructed in optimized operating conditions 12 measurements have been taken by using glucose concentration (5.0 mM) which is in the range of linear determination. Standard deviation and variation coefficient have been calculated as (S.D) ± 0.445 mM ( $n$ : 12) and ( $c_v$ ) 4.84% ( $n$ : 12) respectively using calibration graphics which were plotted in consistence with the measures obtained. LOD value was calculated as 0.903 mM ( $n$ : 5) ( $S/N$ : 3) for P(SNS-NH<sub>2</sub>)/GOx enzyme sensor.

One of most crucial factor limiting practicability of enzyme sensor in various samples is the existence of compounds which will make interference. Ascorbic acid, ethanol, phenolic compounds and other oxidizable compounds generally coexist with glucose in real samples and they likely can interfere the detection of glucose. The interfering effects of, 0.1 mM 3-acetamidophenol, 0.1 mM ethanol, 0.1 mM ascorbic acid in the existence of 5 mM glucose. There was no apparent response after the addition of 0.1 mM 3-acetamidophenol, in the existence of glucose (5.0 mM) as shown in Fig. 11. And also the obtained

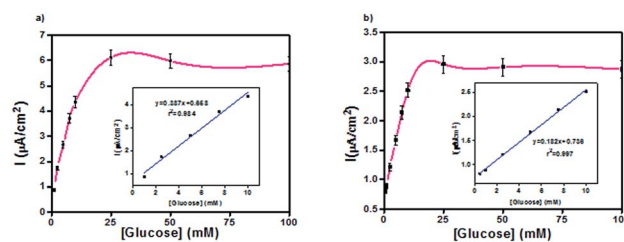


Fig. 10 Calibration curve of (a) P(SNS-NH<sub>2</sub>)/GOx (b) P(SNS-mNH<sub>2</sub>)/GOx enzyme electrode by amperometric detection in Na-acetate buffer.

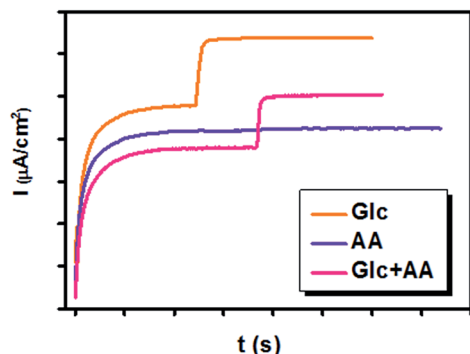


Fig. 11 Amperometric biosensor response of (SNS-NH<sub>2</sub>)/GOx to glucose in the presence of AA.

Table 1 Biosensor response of (SNS-NH<sub>2</sub>)/GOx to glucose in the presence of different compounds

Compound	Biosensor response (μA cm <sup>-2</sup> )	Interference, %
Glucose	2.67 ± 0.02	—
3-AAF	—	—
Glucose + 3-AAF	2.19 ± 0.02	—
Ethanol	—	—
Glucose + ethanol	2.19 ± 0.02	—
Ascorbic acid	—	—
Glucose + ascorbic acid	2.32 ± 0.02	—

Table 2 Glucose analysis results for P(SNS NH<sub>2</sub>)/GOx biosensor and spectrophotometric method in real samples

Sample	Glucose <sup>a</sup> (g L <sup>-1</sup> )		
	Spectrophotometric method	P(SNS-NH <sub>2</sub> )/GOx	Recovery%
Fizzy	20.194 ± 1.987	19.124 ± 1.280	106
Coke	14.286 ± 1.682	14.693 ± 0.513	97

<sup>a</sup> Data were calculated as the average of 3 trials ± S.D.

sensor response to ascorbic acid (0.1 mM), and ethanol (0.1 M) were exhibited in Table 1. These results represent that the constructed P(SNS-NH<sub>2</sub>)/GOx amperometric glucose biosensor has good anti-interference ability and a high selectivity.

Glucose contents in some commercial beverages (coke and fizzy) were determined with P(SNS-NH<sub>2</sub>)/GOx. Determined glucose content values were compared with the values obtained from spectrophotometric method and results were summarized in Table 2.

## 4. Conclusion

As demonstrated in this study, the natures of the isomeric thienylpyrrole derivatives were found to strongly affect the electronic properties of the corresponding electrogenerated conducting polymer films. In particular, the introduction of *p*-

amine in the monomer pattern yielded a more conjugated and more electroactive material compared with those electrogenerated from the *meta* isomer. As a result band gap decrease and improvement of optical contrast were observed for P(SNS-NH<sub>2</sub>). Compared to the spectroelectrochemical properties of the two polymers, P(SNS-NH<sub>2</sub>) has 41.5% and 74.2% optical contrast values at 431 and 834 nm, respectively, whereas, P(SNS-*m*NH<sub>2</sub>) has 25.4% and 54.1% values at 422 and 884 nm, respectively. Polymers have different isomeric structure P(SNS-NH<sub>2</sub>) and P(SNS-*m*NH<sub>2</sub>) were used as first generation amperometric glucose biosensor for enzyme immobilization. Biosensor applications were analyzed for enzyme electrode constructed by P(SNS-NH<sub>2</sub>)/GOx and P(SNS-*m*NH<sub>2</sub>)/GOx. When compared *R* values and the fact that biosensor responses of polymers, (SNS-NH<sub>2</sub>)/GOx based biosensor selected for repeatability, interference determination and sample application tests. We believe that this result is due to steric effect that crosslinking procedures more favourable between glutaraldehyde and P(SNS-NH<sub>2</sub>) to obtain a stable immobilization. Ultimately the biosensor system was accomplished applied for the glucose analysis in the real samples.

## Acknowledgements

Authors gratefully thank the TUBITAK 111T074 grants.

## Notes and references

- 1 A. K. Wanekaya, Y. Lei, E. Bekyarova, W. Chen, R. Haddon, A. Mulchandani and N. V. Myung, *Electroanalysis*, 2006, **18**, 1047–1054.
- 2 T. A. Skotheim, R. L. Elsenbaumer and J. R. Reynolds, *Handbook of Conducting Polymers*, 2007.
- 3 S. Varis, M. Ak, C. Tanyeli, I. M. Akhmedov and L. Toppare, *Eur. Polym. J.*, 2006, **42**, 2352–2360.
- 4 D. Kumar and R. C. Sharma, *Eur. Polym. J.*, 1998, **34**, 1053–1060.
- 5 G. G. Abashev, A. Y. Bushueva and E. V. Shklyueva, *Chem. Heterocycl. Compd.*, 2011, **47**, 130–154.
- 6 A. A. Iyogun, M. R. Kumar and M. S. Freund, *Sens. Actuators, B*, 2015, **215**, 510–517.
- 7 R. M. Sapstead, N. Corden and A. Robert Hillman, *Electrochim. Acta*, 2015, **162**, 119–128.
- 8 W. R. Salaneck, K. Seki, A. Kahn and J. J. Pireaux, *Conjugated Polymer and Molecular Interfaces*, 2001.
- 9 J. Heinze, B. A. Frontana-Urbe and S. Ludwigs, *Chem. Rev.*, 2010, **110**, 4724–4771.
- 10 T. S. El'shina, E. a. Sosnin, E. V. Shklyueva and G. G. Abashev, *Russ. J. Gen. Chem.*, 2013, **83**, 726–730.
- 11 S. Tarkuc, E. Sahmetlioglu, C. Tanyeli, I. M. Akhmedov and L. Toppare, *Sens. Actuators, B*, 2007, **121**, 622–628.
- 12 B. Yigitsoy, S. Varis, C. Tanyeli, I. M. Akhmedov and L. Toppare, *Electrochim. Acta*, 2007, **52**, 6561–6568.
- 13 E. Yildiz, P. Camurlu, C. Tanyeli, I. Akhmedov and L. Toppare, *J. Electroanal. Chem.*, 2008, **612**, 247–256.
- 14 T. Soganci, G. Kurtay, M. Ak and M. Güllü, *RSC Adv.*, 2014, **5**, 2630–2639.

- 15 J. A. Rather, S. Pilehvar and K. De Wael, *J. Nanosci. Nanotechnol.*, 2015, **15**, 3365–3372.
- 16 G. Kaur, R. Adhikari, P. Cass, M. Bown and P. Gunatillake, *RSC Adv.*, 2015, **5**, 37553–37567.
- 17 A. Mulchandani and N. V. Myung, *Curr. Opin. Biotechnol.*, 2011, **22**, 502–508.
- 18 H. S. Nalwa, *Opt. Eng.*, 1997, **36**, 2622.
- 19 J. Njagi and S. Andreescu, *Biosens. Bioelectron.*, 2007, **23**, 168–175.
- 20 Q. Xu, C. Mao, N.-N. Liu, J.-J. Zhu and J. Sheng, *Biosens. Bioelectron.*, 2006, **22**, 768–773.
- 21 S. P. Singh, S. K. Arya, P. Pandey, B. D. Malhotra, S. Saha, K. Sreenivas and V. Gupta, *Appl. Phys. Lett.*, 2007, **91**, 063901.
- 22 Y. Zhang, Y. Shen, D. Han, Z. Wang, J. Song, F. Li and L. Niu, *Biosens. Bioelectron.*, 2007, **23**, 438–443.
- 23 S. Hosseini, F. Ibrahim, I. Djordjevic and L. H. Koole, *Analyst*, 2014, **139**, 2933–2943.
- 24 D. O. Demirkol, H. B. Yildiz, S. Sayin and M. Yilmaz, *RSC Adv.*, 2014, **4**, 19900.
- 25 K. V. Ozdokur, B. Demir, E. Yavuz, F. Ulus, Ç. Erten, İ. Aydın, D. O. Demirkol, L. Pelit, S. Timur and F. N. Ertaş, *Sens. Actuators, B*, 2014, **197**, 123–128.
- 26 T. Soganci, D. O. Demirkol, M. Ak and S. Timur, *RSC Adv.*, 2014, **4**, 46357–46362.
- 27 M. Karadag, C. Geyik, D. O. Demirkol, F. N. Ertas and S. Timur, *Mater. Sci. Eng., C*, 2013, **33**, 634–640.
- 28 N. German, A. Kausaite-Minkstimiene, A. Ramanavicius, T. Semashko, R. Mikhailova and A. Ramanaviciene, *Electrochim. Acta*, 2015, **169**, 326–333.
- 29 H. Ciftci, Y. Oztekin, U. Tamer, A. Ramanaviciene and A. Ramanavicius, *Colloids Surf., B*, 2014, **123**, 685–691.
- 30 V. Krikstolaityte, J. Kuliesius, A. Ramanaviciene, L. Mikoliunaite, A. Kausaite-Minkstimiene, Y. Oztekin and A. Ramanavicius, *Polymer*, 2014, **55**, 1613–1620.
- 31 A. Ramanavicius, P. Genys and A. Ramanaviciene, *Electrochim. Acta*, 2014, **146**, 659–665.
- 32 V. Leskovac, S. Trivić, G. Wohlfahrt, J. Kandrac and D. Pericin, *Int. J. Biochem. Cell Biol.*, 2005, **37**, 731–750.
- 33 G. Oyman, C. Geyik, R. Ayranci, M. Ak, D. Odaci Demirkol, S. Timur and H. Coskunol, *RSC Adv.*, 2014, **4**, 53411–53418.
- 34 R. Ayranci, D. O. Demirkol, M. Ak, and S. Timur, 2015, 1389–1403.
- 35 M. Ak, M. S. Ak, G. Kurtay, M. Güllü and L. Toppare, *Solid State Sci.*, 2010, **12**, 1199–1204.
- 36 G. Sönmez, I. Schwendeman, P. Schottland, K. Zong and J. R. Reynolds, *Macromolecules*, 2003, **36**, 639–647.